NJC

Accepted Manuscript

This article can be cited before page numbers have been issued, to do this please use: P. Liao, G. Cai, J. Shi and J. Zhang, *New J. Chem.*, 2019, DOI: 10.1039/C9NJ00570F.

ROYAL SOCIETY OF CHEMISTRY

rsc.li/njc

View Article Online
DOI: 10.1039/C9NJ00570F

Journal Name

ARTICLE

Post-modified porphyrin imine gels with improved chemical stability and efficient heterogeneous activity in CO_2 transformation

Received 00th January 20xx,
Accepted 00th January 20xx

DOI: 10.1039/x0xx00000x

www.rsc.org/

Peisen Liao, Guangmei Cai, Jianying Shi and Jianyong Zhang*

Efficient heterogeneous gel catalysts have been developed based on dynamic covalent chemistry and post-modification method for chemical fixation of CO_2. Various porphyrin-based imine gels are synthesized and subsequent reduction of imine bonds and metallation with various metal centers yield gel catalysts. The gels are characterized by a number of techniques including SEM, TEM, EDX, FT-IR, CP/MAS ^{13}C NMR, and XPS. The resulting gels not only have networked structures combining micro-, meso- and macropores, but also show improved chemical stability and strong interaction between CO_2 and pore channels. The gel catalysts show good catalytic activity towards cycloaddition of epoxides with CO_2 to cyclic carbonates using wet gels. Post-modified gel catalyst with Zn(II) center (ZnTAPP-Go-r) presents high product yield and high stability with recyclability over 5 cycles.

Introduction

Increasing carbon dioxide level in the atmosphere is leading to the greenhouse effect and global climate change.[1] The conversion of CO_2 into valuable chemicals has attracted much research attention.[2] Cycloaddition of epoxides with CO_2 is one of the important CO_2 transformation reactions.[3] Although homogeneous catalysts, such as ionic liquids,[4-6] phosphonium halides,[7] ammonium[8] and porphyrin complexes,[9-10] have been employed, they are difficult to be separated and reused. Thus heterogeneous catalysts have been developed to solve the problem. Porous materials including porous organic polymers (POPs),[11-17] and MOFs[18-25] are among the most attractive candidates for their high porosity and tuneable structures, which may combine the functions of CO_2 capture, activation and chemical transformation.

Supramolecular gels assembled from small molecules have been developed as a novel type of catalysts because diverse catalytic sites and active organic functional groups can be readily introduced into gelator molecules.[26-30] Different from porous organic polymers[31-33] and metal-organic frameworks,[34] gel catalysts combine both solvent-compatible homogeneous and solid-like heterogeneous advantages.[35,36] For example, we found that dynamic covalent gels with a large specific surface area and hierarchical porosity benefit the adsorption and dissociation of CO_2 molecules and provide convenient mass transfer channels for substrate molecules,[37,38] thus representing a novel catalogue of catalysts for potential application in CO_2 conversion. However, supramolecular gels are generally driven by weak interactions and phase transition may be triggered by heat, light, and other stimuli. The stimuli responsiveness, weak rheology and poor chemical stability of gels have prevented their catalytic applications that require easy recyclability.[39]

Herein, porphyrin-based imine gels and their subsequent post-modification have been studied for CO_2 transformation based on the following considerations. Porphyrin complexes are well known catalysts for cycloaddition of epoxides with CO_2[1,40-43] and other catalytic transformations[44-53] when incorporated in porous networks.[54-57] The porphyrin moiety also provides a platform for further metalation with various catalytically active centres. Post-modification of gels may significantly enhance their mechanical strength, stability, and materials performance whilst keeping the gel morphology.[58-62] First porphyrin-based imine gel is synthesized, then transformed to a amine gel upon the reduction of imine -C=N- bond and further metalated to obtain the gel catalysts. The post-modification and formation of amine moieties not only improve the chemical stability, but also enhances the interaction between CO_2 and the pore channels. Together with the unique networked structure combining micro-, meso- and macropores of imine gels, the modified gels behaves as efficient heterogeneous catalysts using wet gels and can be easily reused in CO_2 fixation to cyclic carbonate.

Results and discussion

A series of metalated porphyrin imine gels were obtained from 5,10,15,20-tetrakis(*p*-amino phenyl) porphyrin (H_2TAPP) based

Sun Yat-Sen University, MOE Laboratory of Polymeric Composite and Functional Materials, Guangzhou 510275, China. Email: zhjyong@mail.sysu.edu.cn.
Electronic Supplementary Information (ESI) available: Experiment details and NMR, MS, SEM, TEM, EDX, IR, XPS, CD and fluorescence data. See DOI: 10.1039/x0xx00000x

View Article Online DOI: 10.1039/C9NJ05705

on dynamic covalent imine chemistry (Scheme 1). H_2TAPP reacted with glyoxal (GO) in a 1:1 molar ratio of $-NH_2$ and –CHO reactive groups in DMSO in the presence of HOAc catalyst. Heating the precursor solution at 80 °C led to the formation of an opaque brown gel H_2TAPP-GO within 4 h, and the gel was thermally irreversible (Fig. 1). For the post-modification method, $NaCNBH_3$ in ethanol was used to reduce the imine bonds of H_2TAPP-GO to -C-N- to obtain H_2TAPP-GO-r gel, and subsequent metalation with $Zn(OAc)_2{\cdot}2H_2O$, $CoCl_2{\cdot}6H_2O$ or $PdCl_2$ achieved MTAPP-GO-r gels (M = Zn, Co and Pd). As control experiments, GO directly reacted with metalated porphyrin (MTAPP) in a 1:1 molar ratio of $-NH_2$ and–CHO reactive groups in DMSO in the presence of HOAc catalyst, yielding MTAPP-GO gels (M = Zn, Co and Pd). Zn, Co and Pd metals were chosen considering the tolerance of functional groups in the material preparation. To characterize the gels, corresponding aerogels were obtained as well by subcritical CO_2(l) drying.[64]

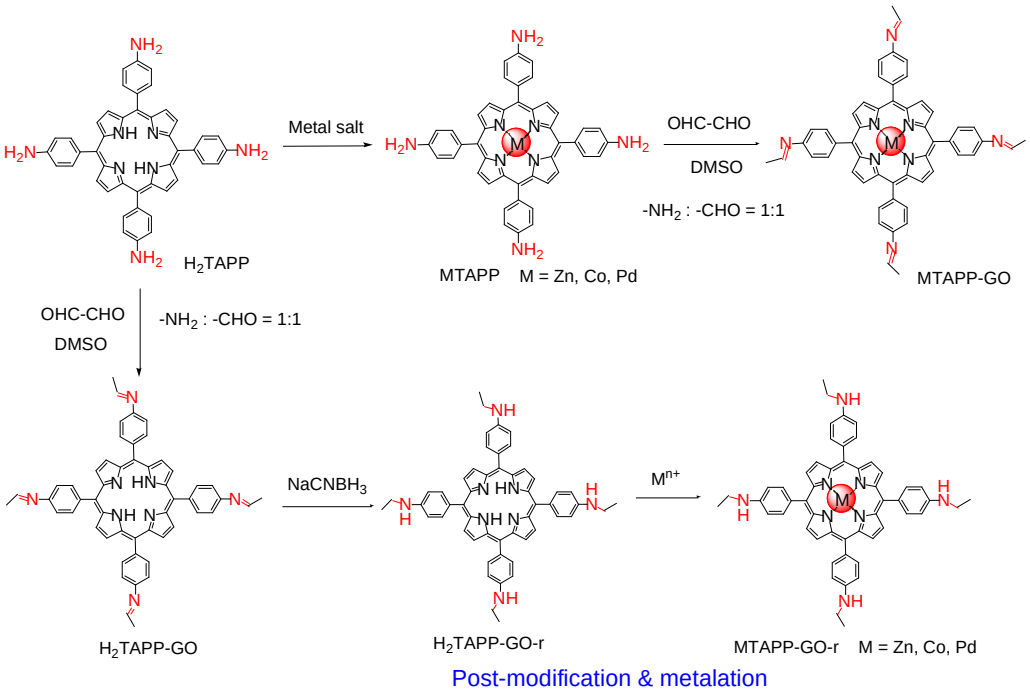

Scheme 1 Synthetic routes to MTAPP-GO and MTAPP-GO-r gels (M = H_2, Zn, Co, Pd).

SEM and TEM investigation shows that the porphyrin-based imine gels have highly porous networked structures consisting of interconnected nanoparticles for H_2TAPP-GO, ZnTAPP-GO, CoTAPP-GO and PdTAPP-GO wet gels (Fig. 2, S1, S2). The particle sizes range around 10-20 nm. The morphologies of post-modified gel H_2TAPP-GO-r, and metalated gels (ZnTAPP-GO-r, CoTAPP-GO-r and PdTAPP-GO-r) are still kept after post-modification and metalation (Fig. 3, S3, S4). The elemental composition of the gels was confirmed by energy dispersive X-ray spectroscopy (EDS) (Fig. S5). All the gel materials are amorphous except that PdTAPP-GO and PdTAPP-GO-r show strong diffraction peaks at 2ϑ around 40° and 46° assigned to polycrystalline Pd as revealed by the broad powder X-ray diffraction patterns (Fig. S6).[64,65]

FT-IR spectra of the imine aerogels display a characteristic Ar–C=N– stretching band at around 1600–1650 cm^{-1} (Fig. S7), confirming the formation of imine bonds via condensation of aldehyde and amine groups. C=O stretching bands of unreacted aldehyde functional groups were detected at around 1665–1700 cm^{-1}, revealing incomplete condensation of aldehyde and amine groups during the gelation. According to the quantitative analysis using FT-IR spectroscopy,[66,67] the percentage of formed Ar–C=N– bonds is 91% for H_2TAPP-GO aerogel (Fig. S8). In comparison with H_2TAPP-GO, H_2TAPP-GO-r shows that the relative intensity of Ar-C=N- stretching band (1614 cm^{-1}) decreases while that of -C-N- (1591 cm^{-1}) increases revealing that the imine bond is reduced to -C-N- by $NaBH_3CN$. The reduction of -C=N- is further confirmed by cross-polarization magic-angle-spinning (CP/MAS) ^{13}C NMR spectra (Fig. 4). For H_2TAPP-GO aerogel, the resonance at around 148.2 ppm is assigned to the imine carbon,[68] while H_2TAPP-GO-r aerogel shows additional peak at 55.0 ppm, which is assigned to -C-N-, supporting the imine bond is reduced.

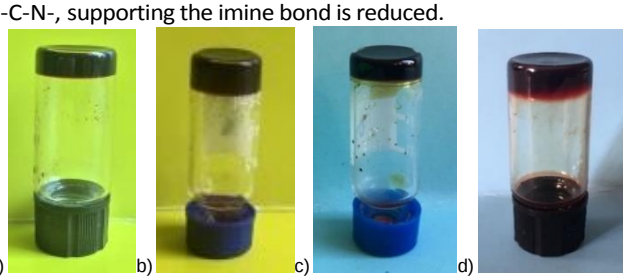

Fig. 1 Photos of a) H_2TAPP-GO, b) ZnTAPP-GO, c) CoTAPP-GO and d) PdTAPP-GO gels.

Solid-state diffuse reflectance UV-vis spectroscopy was used to exploit the Soret band of porphyrin moieties in the gels (Fig. S9). H_2TAPP-GO aerogel has absorption peaks at 426, 525, 567, 600 and 659 nm. After reduction, the absorption peaks do not

change for H_2TAPP-GO-r. While after introduction of transition metal cations, the gels show new absorption peaks (430, 525, 565 and 609 nm for ZnTAPP-GO-r; 439, 550 and 594 nm for CoTAPP-GO-r; 425, 528, 567 and 655 nm for PdTAPP-GO-r). The post-metalated porphyrin gels MTAPP-GO show similar spectra with the corresponding pre-metalated gels MTAPP-GO-r (M= Zn, Co, Pd). Successful metalation of the H_2TAPP-GO-r gel may be supported by the shift of the Soret band and Q bands before and after the metalation.

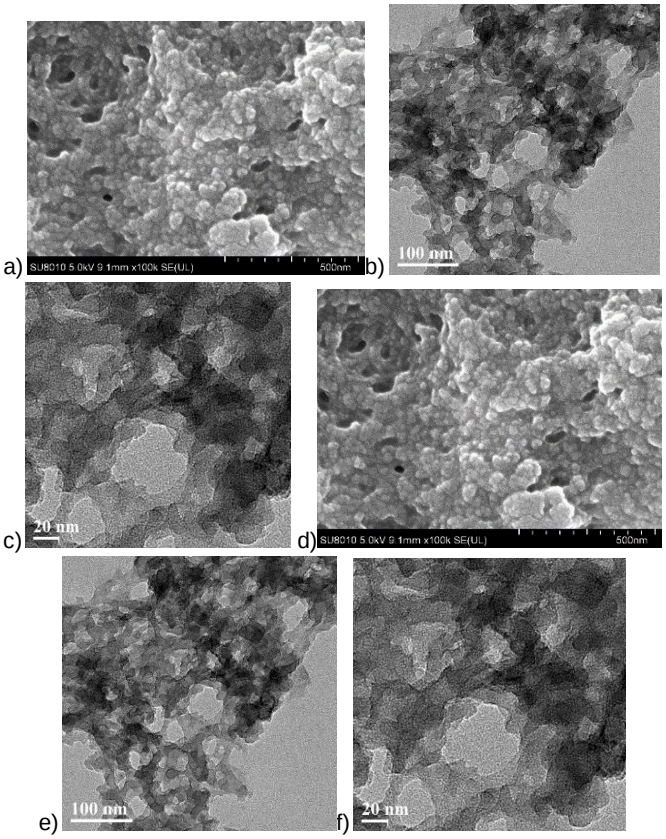

Fig. 2 a) SEM and b,c) TEM images of H_2TAPP-GO gel, and d) SEM and e,f) TEM images of ZnTAPP-GO gel (bars represent 500 nm for SEM).

X-ray photoelectron spectroscopy (XPS) was used to characterize the oxidation states of metal elements in MTAPP-based gels (Fig. S10-S12). For ZnTAPP-GO, peaks of Zn $2p_{1/2}$ and Zn $2p_{3/2}$ were observed with binding energies of 1044.5 and 1021.5 eV, respectively, which is assigned to Zn(II) species.[69,70] ZnTAPP-GO-r also shows similar signals, suggesting Zn^{2+} is embedded inside porphyrin rings successfully by post-modification of H_2TAPP-GO-r. For CoTAPP-GO, Co 2p spectrum shows the signal of Co $2p_{3/2}$ at 780.5 eV and Co $2p_{1/2}$ at 796.5 eV, the Co ($2p_{1/2}$ - $2p_{3/2}$) is 16 eV, which can be assigned to Co(II). While the presence of intense satellite line at 784.6 eV and 802.0 eV revels to the high spin Co^{2+} species. For CoTAPP-GO-r, Co 2p spectrum shows the signals of $Co2p_{1/2}$ and $Co2p_{3/2}$ at 795.7 and 780.4 eV, respectively, the Co ($2p_{1/2}$ - $2p_{3/2}$) is 15.3 eV, which can be assigned to Co(III).[71] For PdTAPP-GO, the fitting of XPS signals confirms the $3d_{3/2}$ and $3d_{5/2}$ states of divalent Pd(II) (binding energies 343.59 and 338.36 eV). For PdTAPP-GO-r, the fitting of XPS signals confirms the $3d_{3/2}$ and $3d_{5/2}$ states of divalent Pd(II) (binding energies 343.59 and 338.36 eV) and Pd(0) (341.00 and 335.78 eV).[72,73] The coexistence of Pd(0) may be due to the reduction of Pd(II) by residue $NaBH_3CN$.

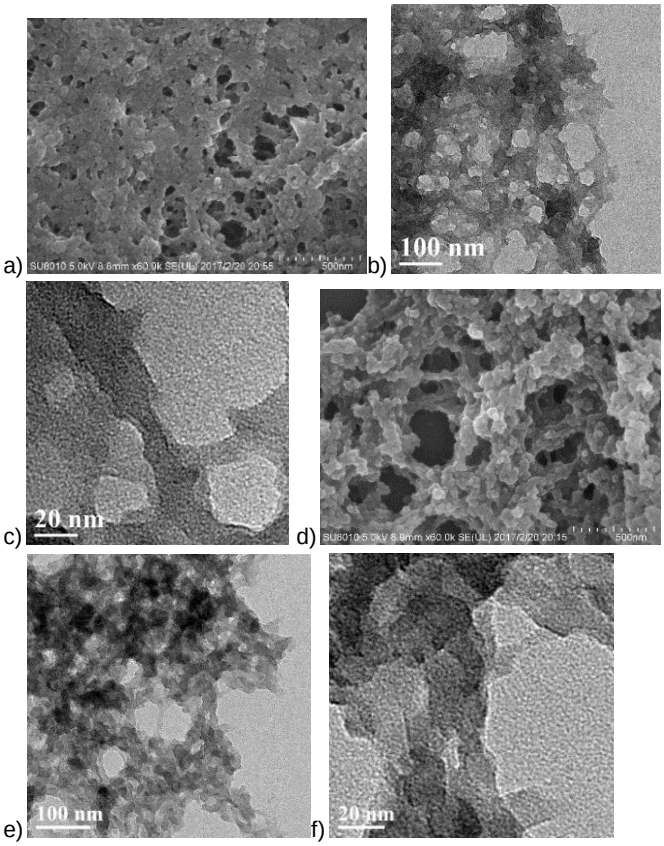

Fig. 3 a) SEM and b,c) TEM images of H_2TAPP-GO-r gel, and d) SEM and e,f) TEM images of ZnTAPP-GO-r gel (bars represent 500 nm for SEM).

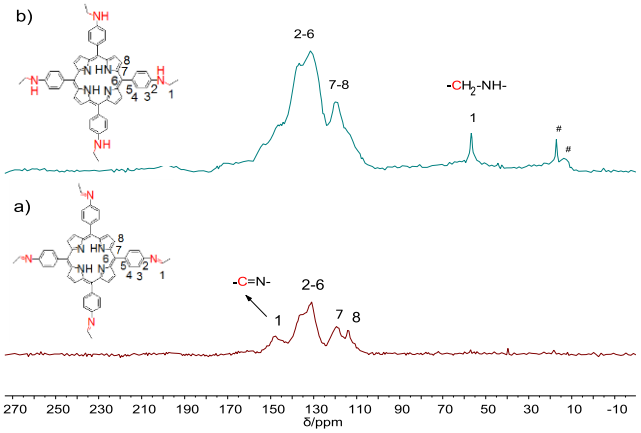

Fig. 4 Solid-state cross-polarization magic-angle-spinning (CP/MAS) ^{13}C NMR spectra of a) H_2TAPP-GO and b) H_2TAPP-GO-r aerogels (signals with # are due to residue ethanol).

The XPS, PXRD and TEM results suggest that no metal nanoparticles are formed for Zn- and Co-based gels, while crystalline Pd nanoparticles appear for Pd-gels during the metalation. The metal weigh percentages of the imine gels

View Article Online DOI: 10.1039/C9NJ00570F

were determined by inductive coupled plasma atomic emission spectroscopy. For ZnTAPP-GO-r, the Zn loading was 83.1 mg g^{-1}, which is close to the theoretical value 82.7 mg g^{-1} (one Zn site in each porphyrin ring).

Additional experiment was performed to test the reactivity of MTAPP-GO and $NaBH_3CN$ (Fig. S10-S12). The resulting XPS spectra show that Zn(II) is kept for ZnTAPP-GO. For PdTAPP-GO, the coexistence of Pd(II) and Pd(0) reveals that a part of Pd(II) in PdTAPP moieties may be reduced to Pd(0) by $NaBH_3CN$. Similarly the coexistence of Co(II) and Co(III) was observed after the reduction of CoTAPP-GO. This suggests that using the pre-metalated MTAPP followed by reduction is an alternative method to the above post-modification method followed by metalation for the formation of MTAPP catalytic centres especially for Zn(II)TAPP catalysts.

Thermostability and adsorption

Thermogravimetric analysis (TGA) shows that H_2TAPP-GO and H_2TAPP-GO-r aerogels have good thermal stability up to 450 °C (Fig. S13). After introduction of metal species, the thermal stability was brought down, and the aerogels were kept stable up to 300 °C. N_2 physisorption was performed at 77 K to characterize the porosity of the porphyrin-based aerogels (Fig. 5, S14-S24, Table S1). H_2TAPP-GO and H_2TAPP-GO-r both show a type II adsorption branch according to the IUPAC classification with a steep rise at p > 0.09 MPa. The isotherms are accompanied by a remarkable hysteresis in the desorption isotherm showing that a range of mesopores are present. The Brunauer-Emmett-Teller (BET) surface area is 261 and 299 m^2 g^{-1}, and the total specific pore volume is 1.75 and 2.88 cm^3 g^{-1} for H_2TAPP-GO and H_2TAPP-GO-r, respectively. Non-local density functional theory (NLDFT) pore size distributions show that the aerogels have a wide range of mesopores. The porosity of H_2TAPP-GO and H_2TAPP-GO-r was also investigated by CO_2 physisorption at 195 K, showing CO_2 adsorption capacity of 100.6 and 74.6 cm^3 g^{-1}, respectively, at 195 K at 1 bar. According to the N_2 physisorption, MTAPP-GO and MTAPP-GO-r aerogels have the BET surface areas of 120-341 m^2 g^{-1} with pore volumes of 0.27-0.97 cm^3 g^{-1}. Among them, PdTAPP-GO-r has the highest specific surface areas (341 m^2 g^{-1}), while PdTAPP-GO has the largest volume of 0.97 cm^3 g^{-1}. The results show that the porosity is generally kept for the gels after the post-modification and metalation process.

CO_2 adsorption was investigated at 273 and 298 K (Fig. 6, S25). H_2TAPP-GO aerogel exhibits CO_2 uptake capacity of 21 cm^3 g^{-1} at 273 K and 11 cm^3 g^{-1} at 298 K, while H_2TAPP-GO-r aerogel has higher CO_2 adsorption capacity of 24.9 and 15.4 cm^3 g^{-1} at 273 and 298 K at 1 bar, respectively. The corresponding isosteric heat of adsorption (Q_{st}) is 46.4 kJ mol^{-1} for H_2TAPP-GO at zero coverage, and lower Q_{st} (39.1 kJ mol^{-1}) for H_2TAPP-GO-r (Table S2, Fig. S26-S29). For metalated MTAPP-GO-r materials, PdTAPP-GO-r shows the highest CO_2 adsorption capacity of 54.6 and 20.4 cm^3 g^{-1} at 273 and 298 K, respectively, at 1 bar. While among MTAPP-GO materials, ZnTAPP-GO shows the highest CO_2 adsorption capacity of 30.5 and 16.8 cm^3 g^{-1} at 273 and 298 K, respectively, at 1 bar. Generally higher Q_{st} (41.6-48.7 kJ mol^{-1}) was observed for MTAPP-GO than those (35.6-41.2 kJ mol^{-1}) for MTAPP-GO-r. The present Q_{st} is higher than those of some imine-based covalent organic frameworks[68,74] and imine-based porous polymers (38.1-27.4 kJ mol^{-1}).[38,76-77] Imine/amine groups and unsaturated coordination metal sites should be responsible for the strong interaction with CO_2.

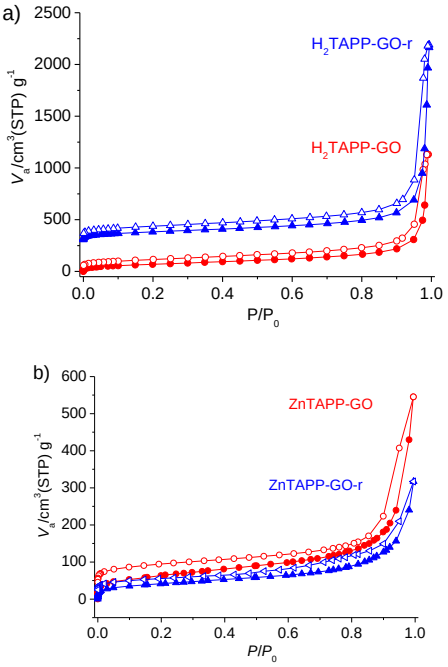

Fig. 5 N_2 adsorption (closed symbols) /desorption (open symbols) isotherms for a) H_2TAPP-GO and H_2TAPP-GO-r aerogels, b) ZnTAPP-GO and ZnTAPP-GO-r aerogels, at 77 K (the isotherms of H_2TAPP-GO-r are vertically offset with 300 cm^3 g^{-1} for clarity).

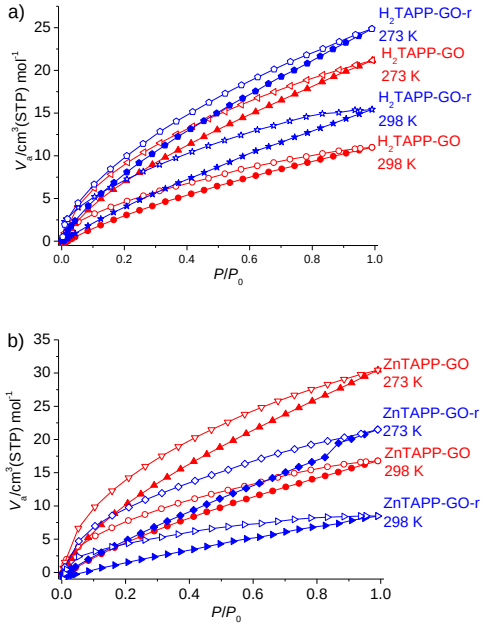

Fig. 6 CO_2 adsorption (closed symbols)/desorption (open symbols) isotherms for a) H_2TAPP-GO and H_2TAPP-GO-r aerogels, b) ZnTAPP-GO and ZnTAPP-GO-r aerogels, at 273 and 298 K.

View Article Online
DOI: 10.1039/C9NJ03705F

Catalytic performance in the cycloaddition of CO_2

The catalytic performance of the porphyrin-based imine gels was evaluated in the cycloaddition of CO_2 with epoxides. The cycloaddition of epoxides with CO_2 was chosen because metalloporphyrin catalysts function as mild Lewis acids in the cycloaddition of CO_2 to epoxides owing to their electron-deficient nature.[40] Meanwhile imine/amine moieties can promote CO_2 binding as shown above. Prior to the reaction the gels were subjected to solvent exchange with DMSO and EtOH in sequence to remove unreacted materials. The cycloaddition of CO_2 and styrene oxide was first investigated as a model reaction to explore the optimized catalytic reaction conditions. Based on the optimization, cycloaddition of styrene oxide was performed with the gel catalysts (1 mol% based on TAPP) under solvent-free conditions in the presence of *n*-Bu_4NBr (TBAB) (7 mol%) as co-catalyst (serving as nucleophilic agent) under atmospheric pressure of CO_2 at 373 K and it was noticed that no reaction occurred without *n*-Bu_4NBr co-catalyst (Table S3). The gels demonstrate highly efficient catalytic activity for the cycloaddition of styrene oxide with CO_2 into styrene carbonate under atmospheric pressure at 373 K. H_2TAPP-GO achieves 99% conversion after 10 h, but with selectivity of only 27%. The selectivity was significantly improved to 75% for H_2TAPP-GO-r. For the MTAPP-GO gels, both ZnTAPP-GO and PdTAPP-GO showed high conversion (~90%) and selectivity (100%) after 10 h. For the MTAPP-GO-r gels, ZnTAPP-GO-r showed high conversion (88%) and selectivity (100%) as well, but CoTAPP-GO-r and PdTAPP-GO-r gave conversion of 43% and 75% after 10 h, with lower selectivity of 31% and 49%, respectively. In these gel catalysts, Zn, Co and Pd metals may act as the Lewis acidic centre to catalyse the cycloaddition of CO_2. The Zn- and Pd-gels show higher activity than the Co-gel which may be due to the weaker Lewis acidity of Co^{3+} than Zn^{2+} and Pd^{2+}.[78-80] However, PdTAPP-GO and PdTAPP-GO-r gels were unstable during the catalysis as revealed by the appearance of Pd(0) after reaction. Therefore ZnTAPP-GO-r gel shows the best stability and catalytic activity toward CO_2 conversion (Fig. 7, Table S4). It is comparable or more efficient than related materials including pyridine-zinc-based porous organic polymer (97% yield in 6 h at 130 °C and 2 bar CO_2),[75] imidazolium-based polymer supported ionic liquids (88% yield in 8 h at 100 °C and 8 bar CO_2),[81] metal-salen-bridged ionic polymer (95% yield in 8h at 80 °C and 0.5 bar CO_2),[78] zinc porphyrin MOFs (53% yield in 14 h at 140 °C and 1 bar CO_2),[18] metalated porous porphyrin polymers (74% yield in 48 h at 50 °C and 1 bar CO_2).[11]

ZnTAPP-GO-r gel was further studied as catalyst for chemical fixation of CO_2 with the epoxides substituted with various functional groups (Table 1, Fig. S30-S34). A wide variety of other terminal epoxide substrates including epoxypropyl phenyl ether, 1,2-epoxyhexane and 1,2-epoxyoctane gave the corresponding cyclic carbonates in excellent conversion (> 88%) under similar conditions. The gel was more active for the cycloaddition of epoxypropyl phenyl ether, and the reaction achieved >99% yield within 10 h. 1,2-Hexanediol and 1,2-octanediol were obtained as main side products for the reaction of 1,2-epoxyhexane and 1,2-epoxyoctane, respectively. In the reaction of epoxycyclohexane, trans-/cis-cyclic carbonate formed with low selectivity (45%) concomitant with the formation of poly(carbonate) and poly(ether).[82,83] Thus ZnTAPP-GO-r was active for the cycloaddition of various epoxide substrates under atmospheric pressure of CO_2 with the general reaction trend, styrene oxide > aliphatic epoxides > cyclohexene oxide.

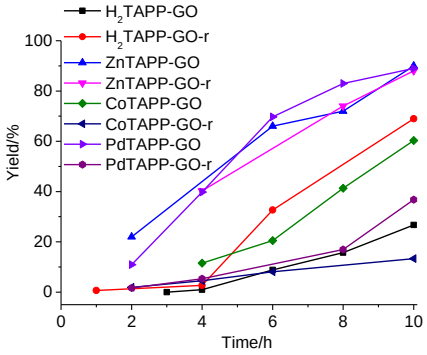

Fig. 7 Catalytic activity of MTAPP-GO and MTAPP-GO-r gels for the conversion of CO_2 and styrene oxide into styrene carbonate. Reaction conditions: 3 mmol styrene oxide, 0.03 mmol of gel catalyst (1 mol% based on TAPP), 0.21 mmol co-catalyst *n*-Bu_4NBr and 1.5 mmol 1-bromo-3,5-dimethylbenzene used as an internal standard at 373 K. The yields were determined by GC and NMR.

Table 1 Catalytic tests of ZnTAPP-GO-r gel for the conversion of CO_2 and epoxides to cyclic carbonates.

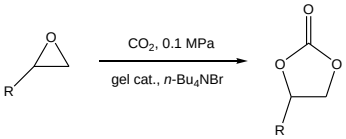

Entry[a]	Epoxide	Cyclic carbonate	Conversion/% (time/h)[b]	Selectivity/% (time/h)[b]
1		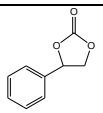	62 (4), 74 (8), 88 (10)	65 (4), 100 (8), 100 (10)
2	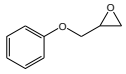	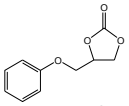	88(4), 91(8), 99 (10)	16 (4), 29 (8), 100 (10)
3	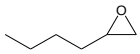	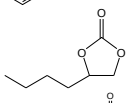	65 (4), 95 (10)	0 (4), 59 (10)
4	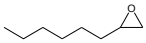	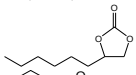	88 (10)	84 (10)
5		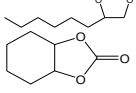	34 (10)	45 (10)

[a] Reaction conditions: 3 mmol epoxide，0.03 mmol of gel catalyst (1 mol% based on TAPP),0.03 mmol of gel catalyst (1 mol% based on H_2TAPP),0.21 mmol co-catalyst *n*-Bu_4NBr and 1.5 mmol 1-bromo-3,5-dimethylbenzene used as an internal standard at 373 K. [b] The conversion and selectivity were determined by GC and NMR analysis. 88 (10) means the conversion is 88% after 10 h and the rest is similar.

To investigate the reusability, ZnTAPP-GO-r and ZnTAPP-GO were examined in the catalytic CO_2 cycloaddition with styrene oxide under similar conditions (Fig. 8, Table S5). The catalysts were readily recovered from the reaction mixture by

View Article Online DOI: 10.1039/C9NJ00570E

centrifugation. ZnTAPP-GO-r showed better stability than ZnTAPP-GO. For ZnTAPP-GO-r, the recovered catalyst could be reused and no significant change was observed in the activity and product yield after five runs. While the activity and product yield of ZnTAPP-GO started to decline after 3 runs. The recycled catalyst ZnTAPP-GO-r was characterized after five runs. SEM and TEM show that the networked gel morphology was generally kept after 5 runs although larger particles (20-50 nm) were formed (Fig. S35). XPS investigation of the recycled gel after five runs showed Zn(II) centres were present and kept the same chemical state (Fig. S36). Furthermore, the Zn weigh percentage in the recovered gel ZnTAPP-GO-r (81.9 mg g^{-1} after 5 runs) was detected to be similar to that of the fresh one (83.1 mg g^{-1}). The improved stability of ZnTAPP-GO-r may be reasonably attributed to the reduction of imine bonds and the formation of C-N single bond. It suggests that the present post-modified strategy efficiently enhance the chemical stability and reusability of supramolecular gel catalysts.

The present gel catalysts are compared with related metalloporphyrin catalysts. ZnTAPP-GO-r shows higher activity than some recently reported metalloporphyrin-based MOFs under similar conditions, including ZnTCPP⊂(Br^-)Etim-UiO-66 (53% yield after 14 h at 140 °C and 1 bar)[18] and MnTPP-MOF (30% yield after 4 h at 80 °C and 1 bar).[21] ZnTAPP-GO-r also shows better activity than some metalloporphyrin porous polymers under similar conditions including SYSU-Zn@IL_2 (80% yield after 12 h at 80 °C and 1 bar)[84] and Co/POP-TPP (74% yield after 48 h at 50 °C and 1 bar).[11] The incorporation of metalloporphyrin and amine moieties into hierarchical cross-linked gel networked structure should be responsible for the activity. The hierarchical pore structure provides convenient mass transfer channels for substrate molecules.

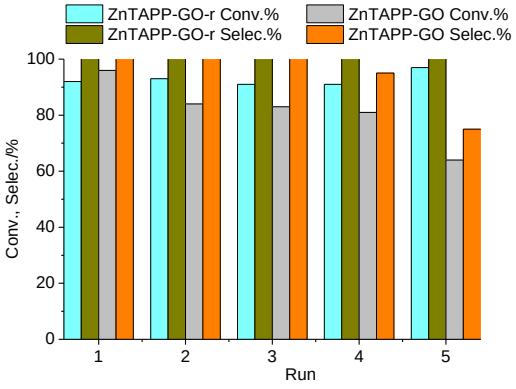

Fig. 8 Recyclability of ZnTAPP-GO-r and ZnTAPP-GO.

Conclusions

In summary, a series of porphyrin/metalloporphyrin imine gels have been successfully synthesized from 5,10,15,20-tetrakis(*p*-amino phenyl) porphyrin and metalated porphyrin (MTAPP, M = Zn, Co and Pd). H_2TAPP-GO has been post-modified to improve its performance. Reducing of the imine bonds of H_2TAPP-GO yielded H_2TAPP-GO-r gel, and subsequent incorporation of metal ions into porphyrin moiety result in MTAPP-GO-r gels (M = Zn, Co and Pd). After post-modification, the morphology and porosity of networked gel structure combining micro-, meso- and macropores are kept as indicated by N_2 adsorption. The dried gel materials display capacity to capture CO_2 (up to 10.7 wt% at 273 K and 1 bar) and exhibit high Q_{st} for CO_2 (up to 48.7 kJ mol^{-1}), indicating the gels has strong affinity with CO_2. The MTAPP-GO and MTAPP-GO-r gels are active in the heterogeneous cycloaddition of epoxides with CO_2 to cyclic carbonates using wet gels. Particularly, ZnTAPP-GO and ZnTAPP-GO-r catalyst shows the best catalytic performance among the catalysts synthesized. The recycling stability of ZnTAPP-GO and ZnTAPP-Go-r reveals that ZnTAPP-GO-r is much more stable during the cycloaddition of epoxides with CO_2 to cyclic carbonates. ZnTAPP-GO-r catalyst can be recycled for at least 5 times without significant decline in activity. This work offers an approach for the design of gel catalysts with tuneable catalytic centres, which feature in both porous gel skeletons and enhanced chemical stability (excellent reusability).

Conflicts of interest

There are no conflicts to declare.

Acknowledgements

We gratefully acknowledge the NSFC (51573216) and the FRF for the Central Universities (16lgjc66) for financial support.

Notes and references

1 S. Wang, K. Song, C. Zhang, Y. Shu, T. Li and B. Tan, *J. Mater. Chem. A*, 2017, **5**, 1509-1515.
2 J. Wu and X. D. Zhou, *Chin. J. Catal.*, 2016, **37**, 999-1015.
3 S. Jayakumar, H. Li, J. Chen and Q. Yang, *ACS Appl. Mat. Interfaces*, 2018, **10**, 2546-2555.
4 Z. Z. Yang, L. N. He, C. X. Miao and S. Chanfreau, *Adv. Synth. Catal.*, 2010, **352**, 2233-2240.
5 M. Liu, L. Liang, X. Li, X. Gao and J. Sun, *Green Chem.*, 2016, **18**, 2851-2863.
6 J. Xu, M. Xu, J. Wu, H. Wu, W. H. Zhang and Y. X. Li, *RSC Adv.*, 2015, **5**, 72361-72368.
7 Q. Sun, Y. Jin, B. Aguila, X. Meng, S. Ma and F. S. Xiao, *ChemSusChem*, 2017, **10**, 1160-1165.
8 C. C. Rocha, T. Onfroy, J. Pilmé, A. Denicourt-Nowicki, A. Roucoux and F. Launay, *J. Catal.*, 2016, **333**, 29-39.
9 C. Maeda, T. Taniguchi, K. Ogawa and T. Ema, *Angew. Chem. Int. Ed.*, 2015, **54**, 134-138.
10 C. Maeda, S. Sasaki and T. Ema, *ChemCatChem*, 2017, **9**, 946-949.
11 Z. Dai, Q. Sun, X. Liu, C. Bian, Q. Wu, S. Pan and F. S. Xiao, *J. Catal.*, 2016, **338**, 202-209.
12 Z. D. Ding, W. Zhu, T. Li, R. Shen, Y. Li, Z. Li and Z. G. Gu, *Dalton Trans.*, 2017, **46**, 11372-11379.
13 W. Wang, C. Li, L. Yan, Y. Wang, M. Jiang and Y. Ding, *ACS Catal.*, 2016, **6**, 6091-6100.
14 F. Liu, K. Huang, Q. Wu and S. Dai, *Adv. Mater.*, 2017, **29**, 1700445.
15 W. G. Lu, D. Q. Yuan, J. Sculley, D. Zhao, R. Krishna and H. C. Zhou, *J. Am. Chem. Soc.*, 2011, **133**, 18126-18129.
16 Q. Sun, B. Aguila, J. Perman, N. Nguyen and S. Ma. *J. Am. Chem. Soc.*, 2016, **138**, 15790-15796.

17 G. P. Ji, Z. Z Yang, H. Y. Zhang, Y. F. Zhao, B. Yu, Z. S. Ma and Z. M. Liu, *Angew. Chem. Int. Ed.*, 2016, **55**, 9685-9689.
18 J. Liang, Y. Q. Xie, Q. Wu, X. Y. Wang, T. T. Liu, H. F. Li and R. Cao, *Inorg. Chem.*, 2018, **57**, 2584-2593.
19 W. Y. Gao, H. Wu, K. Leng, Y. Sun and S. Ma, *Angew. Chem. Int. Ed.*, 2016, **55**, 5472-5476.
20 L. Zhang, J. Liu, Y. Z. Fan, X. Li, Y. W. Xu and C. Y. Su, *ChemSusChem*, 2018, **11**, 2340-2347.
21 W. Jiang, J. Yang, Y. Y. Liu, S. Y. Song and J. F. Ma, *Chem. Eur. J.*, 2016, **22**, 16991-16997.
22 W. Y. Gao, C. Y. Tsai, L. Wojtas, T. Thiounn, C. C. Lin and S. Ma. *Inorg. Chem.*, 2016, **55**, 7291-7294.
23 H. H. Wang, L. Hou, Y. Z. Li, C. Y. Jiang, Y. Y. Wang and Z. Zhu, *ACS Appl. Mat. Interfaces*, 2017, **9**, 17969-17976.
24 Z. Zhou, C. He, J. Xiu, L. Yang and C. Duan, *J. Am. Chem. Soc*., 2015, **137**, 15066-15069.
25 P. Z. Li, X. J. Wang, J. Liu, J. S. Lim, R. Zou and Y. Zhao, *J. Am. Chem. Soc*., 2016, **138**, 2142-2145.
26 W. Fang, Y. Zhang, J. Wu, C. Liu, H. Zhu and T. Tu, *Chem. Asian J*., 2018, **13**, 712-729.
27 L. Liu, J. Zhang, H. Fang, L. Chen and C. Y. Su, *Chem. Asian J*., 2016, **11**, 2278-2283.
28 S. Chen, X. Lin, Z. Zhai, R. Lan, J. Li, Y. Wang, S. Zhou, Z. H. Farooqi and W. Wu, *Polym. Chem.*, 2018, **9**, 2887-2896.
29 M. V. Alekseeva, M. A. Rekhtina,M. Y. Lebedev, S. G. Zavarukhin, V. V. Kaichev, R. H. Venderbosch and V. A. Yakovlev, *ChemistrySelect*, 2018, **3**, 5153-5164.
30 H. Liu, J. Feng, J. Zhang, P. W. Miller, L. Chen and C. Y. Su, *Chem. Sci.*, 2015, **6**, 2292-2296.
31 S. Kramer, N. R. Bennedsen and S. Kegnæs, *ACS Catal.*, 2018, **8**, 6961−6982.
32 P. Bhanja, A. Modak and A. Bhaumik, *ChemCatChem*, 2018, **10**, 1-5.
33 K. Huang, J. Y. Zhang, F. Liu and S. Dai, *ACS Catal.*, 2018, **8**, 9079−9102.
34 Z. Zhou, L. Yang, Y. Wang, C. He and C. Duan, *Curr. Org. Chem.*, 2018, **22**, 1809-1824.
35 J. Zhang and S. L. James, in *Homogeneous Catalysts: Types, Reactions and Applications*, (Ed.: A. C. Poehler), Nova Science, New York, 2011, pp. 155-184.
36 B. Escuder and F. Rodríguez-Llansola and J. F. Miravet, *New J. Chem.*, 2010, **34,** 1044-1054.
37 L. Zeng, P. Liao, H. Liu, Z. Liang, J. Zhang, L. Chen and C. Y. Su, *J. Mater. Chem. A*, 2016, **4**, 8328-8336.
38 J. Zhang, L. Liu , H. Liu , M. Lin , S. Li , G. Ouyang, L. Chen and C. Y. Su, *J. Mater. Chem. A*, 2015, **3**, 10990-10998.
39 P. Slavík, D. W. Kurka and D. K. Smith, *Chem. Sci.*, 2018, **9**, 8673-8681.
40 A. Chen, Y. Zhang, J. Chen, L. Chen and Y. Yu, *J. Mater. Chem. A*, 2015, **3**, 9807–9816.
41 S. Jayakumar, H. Li, J. Chen and Q. Yang, *ACS Appl. Mater. Interfaces*, 2018, **10**, 2546-2555.
42 X. Sheng, H. Guo, Y. Qin, X. Wang and F. Wang, *RSC Adv.*, 2015, **5**, 31664–31669.
43 J. Chen, M. Zhong, L. Tao, L. Liu, S. Jayakumar, C. Li, H. Li and Q. Yang, *Green Chem.*, 2018, **20**, 903–911.
44 A. M. Shultz, O. K. Farha, J. T. Hupp and S. T. Nguyen, *Chem. Sci.*, 2011, **2**, 686–689.
45 L. Chen, Y. Yang, Z. Guo and D. Jiang, *Adv. Mater.*, 2011, **23**, 3149–3154.
46 D. B. Shinde, S. Kandambeth, P. Pachfule, R. R. Kumar and R. Banerjee, *Chem. Commun.*, 2015, **51**, 310-313.
47 S. Lin, C. S. Diercks, Y. B. Zhang, N. Kornienko, E. M. Nichols, Y. B Zhao, A. R. Paris, D. Kim, P. D. Yang, O. M. Yaghi and C. J. Chang, *Science*, 2015, **349**, 1208-1213.
48 J. Yoo, N. Park, J. H. Park, J. H. Park, S. Kang, S. M. Lee, H. J. Kim, H. Jo, J. G. Park and S. U. Son, *ACS Catal.*, 2015, **5**, 350−355.
49 A. Modak, M. Pramanik, S. Inagakibc and A. Bhaumik, *J. Mater. Chem. A*, 2014, **2**, 11642–11650.
50 A. Modak, J. Mondal and A. Bhaumik, *Appl. Catal. A Gen.*, 2013, **459**, 41-51.
51 X. M. Liu, A. Sigen, Y. W. Zhang, X. L. Luo, H. Xia, H. Li and Y. Mu, *RSC Adv.*, 2014, **4**, 6447-6453.
52 Y. Li, B. Sun and W. Yang, *Appl. Catal. A Gen.*, 2016, **515**, 164-169.
53 Y. Li, B. Sun, Y. Zhou and W. Yang, *Appl. Organomet. Chem.*, 2017, **31**, e3578.
54 J. Xia, S. Yuan, Z. Wang, S. Kirklin, B. Dorney, D. J. Liu and L. Yu, *Macromolecules*, 2010, **43**, 3325-3330.
55 A. Modak, M. Nandi, J. Mondal and A. Bhaumik, *Chem. Commun.*, 2012, **48**, 248-250.
56 S. Kandambeth, D. B. Shinde, M. K. Panda, B. Lukose, T. Heine and R. Banerjee, *Angew. Chem. Int. Ed.*, 2013, **52**, 13052-13056.
57 Q. Lin, J. Lu, Z. Yang, X. C. Zeng and J, Zhang, *J. Mater. Chem. A*, 2014, **2**, 14876-14882.
58 I. A. Coates and D. K. Smith, *Chem. Eur. J*., 2009, **15**, 6340-6344.
59 D. J. Cornwell and D. K. Smith, *Mater. Horiz.*, 2015, **2**, 279-293.
60 H. Zhao, Q. Xie, X. Ding, J. Chen, M. Hua, X. Tan and Y. Zhang, *J. Memb. Sci.*, 2016, **514**, 305-312.
61 S. Sanda, K. Kanamori, T. Takei and K. Tashiro, *ChemNanoMat*, 2018, **4**, 52-55.
62 K. Thiel, R. Zehbe, J. Roeser, P. Strauch, S. Enthaler and A. Thomas, *Polym. Chem.*, 2013, **4**, 1848-1856.
63 L. Li, S. Xiang, S. Cao, J. Zhang, G. Ouyang, L. Chen and C. Y. Su, *Nat Commun*., 2013, **4**, 1774.
64 Z. Ferhat-Hamida, J. Barbier Jr, S. Labruquere and D. Duprez, *Appl. Catal. B*, 2001, **29**, 195-205.
65 T. Maillet, C. Solleau, J. Barbier Jr and D. Duprez, *Appl. Catal. B*, 1997, **14**, 85-95.
66 N. V. Vagenas, A. Gatsouli and C. G. Kontoyannis. *Talanta*, 2003, **59**, 831-836.
67 T. Buffeteau, B. Dsbat and J. M. Turlet. *Appl. Spectroscopy*, 1991, **45**,380-389.
68 M. G. Rabbani, A. K. Sekizkardes, Z. Kahveci, T. E. Reich, R. Ding and H. M. El-Kaderi, *Chem. Eur. J.*, 2013, **19**, 3324-3328.
69 R. Zeng, G. Chen, C. Xiong, G. Li, Y. Zheng, J. Chen, Y. Long and S. Chen, *Appl. Surf. Sci.*, 2018, **434**, 756-762.
70 Q. Wu, K. Huang, F. Liu, P. Zhang and L. Jiang, *Ind. Eng. Chem. Res.*, 2017, **56**, 15008-15016.
71 J. W. Murray and J. G. Dillard, *Geochim. Cosmochim. Acta*., 1979, **43**, 781-787.
72 P. Sharma and A. P. Singh, *RSC Adv.*, 2014, **4**, 58467-58475.
73 Y. Luo, J. Zuo, X. Feng, Q. Qian, Y. Zheng, D. Lin, B. Huang and Q. Chen, *Chem. Eng. J*., 2018, **357**, 1385-8947.
74 Y. Zhu, H. Long and W. Zhang, *Chem. Mater.*, 2013, **25**, 1630-1635.
75 H Li, C. Li, J. Chen, L. Liu and Q. Yang, *Chem. Asian J.*, 2017, **12**, 1095-1103.
76 H. S. Jena, C. Krishnaraj, G. Wang, K. Leus, J. Schmidt, N. Chaoui and P. van der Voort, *Chem. Mater.*, 2018, **30**, 4102-4111.
77 G. Chang, Y. Xu, L. Zhang and L. Yang, *Polym. Chem.*, 2018, **9**, 4455-4459.
78 C. Zhang, D. Lu, Y. Leng and P. Jiang, *Mol. Catal.*, 2017, **439**, 193-199.
79 Y. Chen, R. Luo, Z. Yang, X. Zhou and H. Ji, *Sustainable Energy Fuels*, 2018, **2**, 125-132.
80 T. T. Wang, Y. Xie and W. Q. Deng, *J. Phys. Chem. A*, 2014, **118**, 9239-9243.
81 A. H. Jadhava, G. M. Thorat, K. Le, A. C. Lim and H. K. J. G. Seo, *Catal. Today*, 2016, **265**, 56-67.

View Article Online
DOI: 10.1039/C9NJ00570F

82 P. Gao, Z. Zhao, L. Chen, D. Yuan and Y. Yao, *Organometallics*, 2016, 35, 1707-1712.
83 M. Cozzolino, K. Press, M. Mazzeo and M. Lamberti, *ChemCatChem*, 2016, **8**, 455-460.
84 Y. Chen, R. Luo, Q. Xu, J. Jiang, X. Zhou and H. Ji. *ACS Sustainable Chem. Eng.*, 2018, **6**, 1074−1082.

View Article Online
DOI: 10.1039/C9NJ00570F

Table of Contents

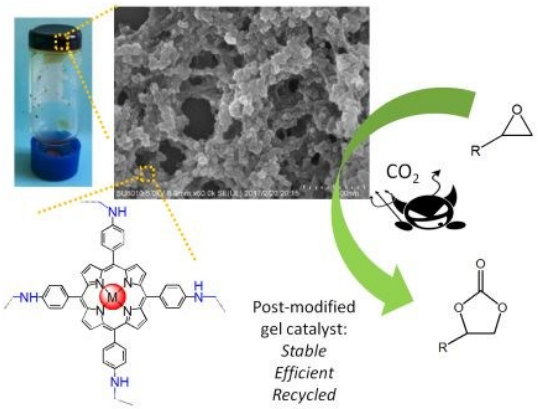

Gel catalysts have been developed based on dynamic covalent chemistry and post-modification method for improved chemical stability and catalytic activity.